Pergamon

0022-4073(95)00062-3

J. Quant. Spectrosc. Radiat. Transfer Vol. 54, No. 1/2, pp. 261–269, 1995

0022-4073/95 $9.50 + 0.00

EXCITATION–AUTOIONIZATION, DIELECTRONIC RECOMBINATION AND LINE INTENSITIES IN HIGHLY IONIZED CuI-LIKE IONS

P. MANDELBAUM, D. MITNIK, E. BEHAR, R. DORON, and J. L. SCHWOB

Racah Institute of Physics, The Hebrew University, 91904 Jerusalem, Israel

Abstract—Extended calculations for excitation–autoionization processes in the CuI isoelectronic sequence and for dielectronic recombination in the NiI sequence have been performed. As an example, the results of these computations for molybdenum ions are presented. On the basis of these results one interprets the unexpected weak intensities of the CuI-like Mo XIV $3d^{10}4s$–$3d^{9}4s4f$ resonant transitions compared to the parent Mo XV $3d^{10}$–$3d^{9}4f$ transitions.

INTRODUCTION

In recent years there has been an increasing interest in atomic data for ions with $3d^{x}4l^{y}$ outer electrons. This has been related, among other things, to the development of X-ray lasers based on population inversion in NiI-like ions[1] and the use of $3d$–$4l$ emission for producing X-ray quasi-continuum bands.[2,3] On the other hand, few atomic data have been published or are available for ions pertaining to these isoelectronic sequences. In particular, there is a definite lack of systematic calculations for electron impact ionization and dielectronic recombination which are crucial for ionization balance computations. As a first step, excitation–autoionization (EA) processes through $3d$–$4l$ inner-shell excitations have been studied for ions in the isoelectronic sequences from CuI to KrI.[4] As a second step, more complete calculations for EA processes for CuI-like ions via other configurations have been recently undertaken. Also, computations for dielectronic recombination (DR) processes from NiI- to CuI-like ions and a systematic study of the line intensity of the $3d^{10}4s$–$3d^{9}4s4f$ transitions have been performed. The $3d^{9}4s4f$ configuration in the present work denotes, in fact, the mixed $3d^{9}[4s4f + 4p4d]$ configurations. In the present paper, an overview of the results is given with an emphasis on the molybdenum ions which are taken as a case study.

THEORETICAL METHODS

The present calculations were performed with the HULLAC computer package.[5] These codes include the RELAC code for atomic energy levels and radiative transition rate calculations,[6] which has been recently extended to include radiationless autoionization transitions.[7] The electron collision excitation rates are calculated using the efficient CROSS code[8] which is based on the factorization interpolation method.

GENERAL ISOELECTRONIC SEQUENCE TREND

Many of the properties of the isoelectronic sequences with ground state $3d^{10}4s^{x}4p^{y}$ ($x = 1, 2, y = 0$; $x = 2, y = 1$–6) can be tested through the study of the simpler CuI sequence (ground state $3d^{10}4s$). For this sequence detailed calculations for EA and dielectronic recombination (DR) processes are now close to being achieved. Preliminary results for molybdenum are given and discussed here. An important conclusion of our set of calculations is that, for the processes involved

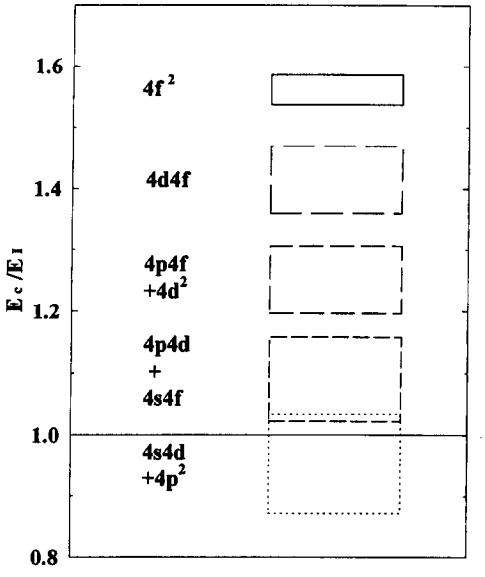

Fig. 1. Energy E_C of the inner-shell excited configurations within the $3d^9 4l 4l'$ complex relative to the first ionization limit E_I for CuI-like Mo XIV. The energies are indicated by a finite vertical range representing the full level spread within each configuration.

here, one can neither make valid interpolations for one element from detailed results for other elements, nor use configuration averaging methods. Instead, one has to perform detailed intermediate coupling calculations for every element. The main reason for this is that the first ionization limit lies in the middle of the $3d^9 4l 4l'$ configuration complex and, thus, the number of levels in this complex contributing to EA or DR processes changes from element to element. Moreover, this complex in fact gives the most important contribution to the EA and DR processes. For the same reason, one cannot use averaged atomic quantities (e.g. electron impact excitations, radiative decay and autoionization rates) over a whole configuration, since in many cases one part of the configuration lies above the ionization limit while the other part lies below. This fact is illustrated in Fig. 1 which shows the relative position of the $3d^9 4l 4l'$ configurations (or mixed configurations) around the ionization limit for CuI-like Mo XIV. Apart from the configurations $3d^9 4s^2$, $3d^9 4s 4p$ (not shown in Fig. 1) and $3d^9 4p^2$, all the other configurations of the complex lie above the ionization limit. However, this picture gradually changes as a function of Z. For CuI-like Uranium, for instance, all the configurations of the $3d^9 4l 4l'$ complex are below the ionization limit, except for the $3d^9 4f^2$ configuration.

EXCITATION–AUTOIONIZATION

The total cross section σ^{EA} for EA from the ground level g ($3d^{10}4s$) of the CuI-like ion to any level k of the NiI-like ion, through inner-shell excitation of the CuI-like ion to any intermediate autoionizing level j within a given configuration or complex C is given by:

$$\sigma_C^{EA}(E) = \sum_{J \in C} \left[\frac{\sigma_{gj}(E) \sum_k A_{jk}^a}{\sum_k A_{jk}^a + \sum_i A_{ji}} \right] \tag{1}$$

where, $\sigma_{gj}(E)$ is the cross section for electron impact excitation from level g to the inner-shell excited level j as a function of the incident electron kinetic energy E. A_{jk}^a is the rate coefficient for autoionization from level j to a level k of the NiI-like ion. In the present work k is mostly the $3d^{10}$ ground state of the NiI-like ion, although autoionization to $3d^9 4s$ is energetically allowed in some cases. A_{ji} is the Einstein coefficient for spontaneous emission from level j to any lower lying CuI-like level i. Figure 2 shows the results for the EA cross section for Mo XIV as a function of the electron

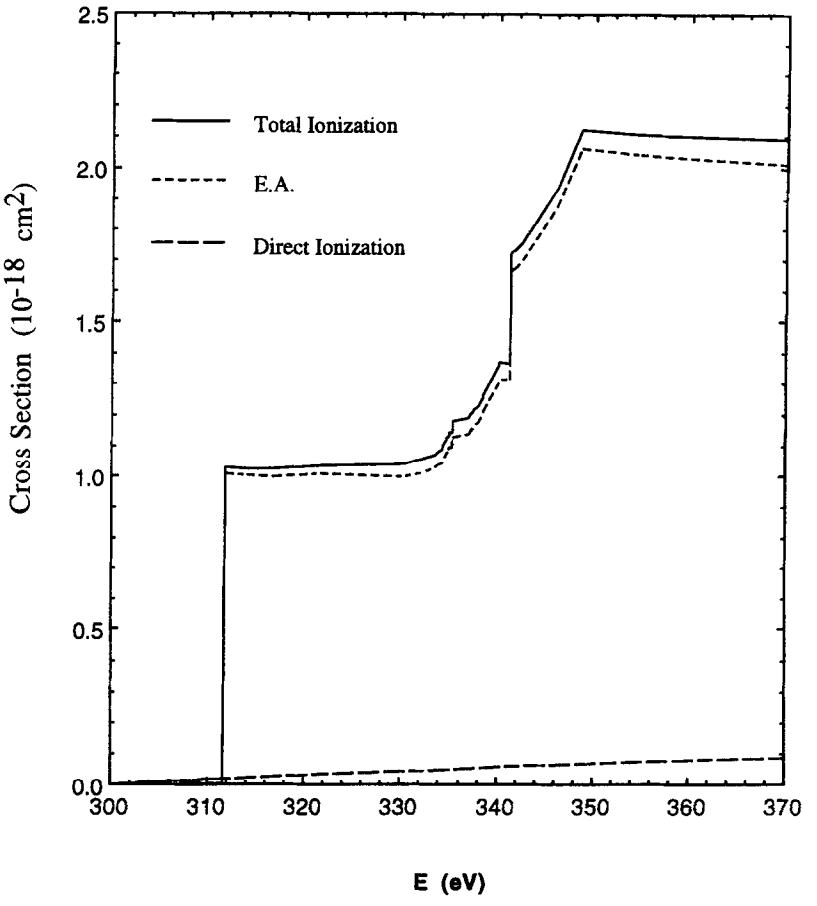

Fig. 2. Ionization cross section of Mo XIV as a function of the incident electron kinetic energy. The solid curve is the total cross section, whereas the dotted and dashed curves represent the EA and direct ionization cross sections, respectively.

impact energy in the 300–370 eV range. In this energy range the total EA cross section is almost two orders of magnitude greater than the direct ionization cross section as obtained from the approximate Lotz formula.[9] The steep increase in the EA cross section is due to $3d^{10}4s$–$3d^9 4s4d$ and $3d^{10}4s$–$3d^9 4s4f$ excitations.

Assuming a Maxwellian velocity distribution $f(v)$ for the electrons, one can compute the rate coefficient S_C^{EA} for EA as a function of the electron temperature T_e:

$$S_C^{EA} = \int_0^\infty \sigma_C^{EA}(v) v f(v)\, dv. \tag{2}$$

Table 1 gives the computation results of the EA rate coefficients for Mo XIV at four electron temperatures (in ionization energy units). The second row gives the direct ionization rate coefficient S^D calculated by the Lotz formula taking into account the ionizations from the three outer shells. The next rows give the partial contribution of the most important EA transitions. The two last rows give the total EA rate coefficient and the ratio of this rate to the direct ionization rate. By extrapolating the results for $3d$–nl excitations with $n \leqslant 7$ we could estimate the contribution of the excitations for $n = 8$ to ∞. This showed that the contribution of the latter could be neglected. All the computations were carried out with full intermediate coupling calculations including configuration mixings. Also, autoionization processes following radiative decays were taken into account. The results clearly show the predominance of EA processes on direct ionization in the relevant T_e range.

DIELECTRONIC RECOMBINATION

The rate coefficient β_{kj} for the capture of a free electron by a NiI-like ion in the level k (assumed here to be the ground state) to form a CuI-like ion in an inner-shell excited level j is given by:

$$\beta_{kj} = 1.65 \times 10^{-22}(kT_e)^{-3/2}\frac{g_j}{g_k}A^a_{jk}\exp[-(\Delta E_j/kT_e)] \tag{3}$$

where $\Delta E_j = E_j - E_1$ is the kinetic energy of the incident free electron (E_j and E_1 are the energy of level j and the first ionization energy of the CuI-like ion, respectively). ΔE_j and kT_e are expressed in eV. g_k and g_j are the statistical weights of the k and j levels, respectively. β_{kj} is expressed in $cm^3\,s^{-1}$. Neglecting electron collisions in the j level depopulation processes, the rate coefficient for *effective* dielectronic recombination (i.e., electron capture followed by radiative stabilization) from the ground level k of the NiI-like ion to any level i of the CuI-like ion through a given autoionizing level j is:

$$\alpha^D_{kj} = \beta_{kj}\frac{\sum_i A_{ji}}{\sum_{k'} A^a_{jk'} + \sum_i A_{ji}}. \tag{4}$$

As for the EA rates from CuI-like to NiI-like ions, the DR rates from the NiI-like ground level into CuI-like levels are essentially determined, particularly in the lower to intermediate T_e range, by the positions of the energy levels of the $3d^9 4l 4l'$ complex relative to the ionization limit. For Mo XV ions, dielectronic recombination to Mo XIV is possible through 599 levels of this complex. For U LXV, only 115 of these levels can still contribute to DR processes. For this reason one must also perform DR computations using detailed level-by-level computations. Further, configuration interaction can be very important because of the opening of radiative decay channels which

Table 1. Computed EA rate coefficients for Mo XIV at four electron temperatures. $E_1 = 301$ eV is the first ionization energy. The direct ionization rate coefficient was obtained by using the Lotz formula and taking into account the direct ionization of $4s$, $3d$ and $3p$ bound electrons. The rate coefficients are given in $cm^3\,s^{-1}$. $X[-Y]$ denotes $X \times 10^{-Y}$.

T_e		$0.3E_1$	$0.5E_1$	$0.7E_1$	$1.E_1$
S^D		1.27[-11]	8.23[-11]	2.04[-10]	4.33[-10]
S_c^{EA}	3d-4l	1.43[-10]	4.94[-10]	8.10[-10]	1.14[-9]
	3d-5l	2.46[-11]	1.12[-10]	2.05[-10]	3.13[-10]
	3d-6l	6.83[-12]	3.65[-11]	7.17[-11]	1.15[-10]
	3d-7l	2.76[-12]	1.64[-11]	4.36[-11]	5.60[-11]
	3p-4l	1.22[-11]	6.36[-11]	1.24[-10]	1.96[-10]
	3p-5l	9.77[-13]	8.49[-12]	2.04[-11]	3.79[-11]
S^{EA}total		1.91[-10]	7.31[-10]	1.27[-9]	1.86[-9]
S^{EA}/S^D		15.3	8.9	6.2	4.3

Table 2. Computed DR rate coefficients for Mo XV at five electron temperatures. The rate coefficients are given in $cm^3 s^{-1}$. $X[-Y]$ denotes $X \times 10^{-Y}$.

	T_e (eV)				
COMPLEX	20	40	100	200	1000
$3d^9 4l4l'$	1.87[-11]	2.66[-11]	2.27[-11]	1.33[-11]	1.85[-12]
$3d^9 4l5l'$	6.71[-13]	4.92[-12]	1.46[-11]	1.34[-11]	2.67[-12]
$3d^9 4f6l'$	8.13[-16]	2.28[-13]	3.26[-12]	4.44[-12]	1.17[-12]
$3d^9 4f7l'$	2.34[-16]	1.23[-13]	2.51[-12]	3.85[-12]	1.11[-12]
$3d^9 4f8l'$	4.89[-17]	3.87[-14]	1.00[-12]	1.66[-12]	5.10[-13]
$3p^5 4l4l'$	1.65[-13]	9.90[-13]	3.10[-12]	3.06[-12]	6.61[-13]
$3p^5 4l5l'$	6.41[-17]	6.30[-15]	7.33[-14]	1.05[-13]	3.04[-14]
$3s^1 4l4l'$	2.88[-16]	3.31[-14]	4.50[-13]	6.76[-13]	2.00[-13]
$3s^1 4l5l'$	1.02[-19]	2.88[-16]	1.84[-14]	4.23[-14]	1.71[-14]
Total	1.95[-11]	3.31[-11]	5.25[-11]	4.87[-11]	1.08[-11]

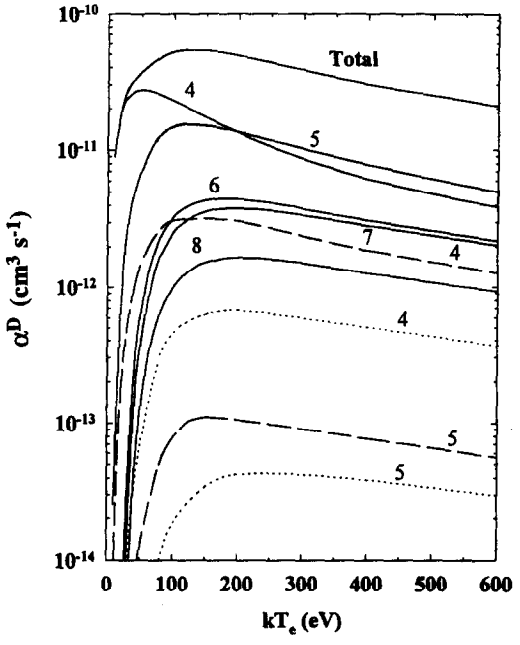

Fig. 3. Total and partial rate coefficients for DR of Mo XV through various CuI-like configuration complexes as a function of the electron temperature. The solid curves indicate the $3d^9 4ln'l'$ complexes, the labels 4 to 8 represent the value of n'. For $n' = 6$, 7 and 8 only $l = 3$ was included. The dashed curves indicate the $3s^2 3p^5 3d^{10} 4ln'l'$ complexes, the labels 4 and 5 representing the n' values. The dotted curves indicate the $3s 3p^6 3d^{10} 4ln'l'$ complexes, the labels 4 and 5 representing here also the n' values.

otherwise would not be allowed (e.g., $3d^9 4d^2$ can decay to $3d^{10}4p$ or $3d^{10}4f$ through the mixing with $3d^9 4p 4f$). Table 2 shows the results of the DR computations for Mo XV. The partial contributions of the different complexes taken into account are given. The last row gives the total DR rate coefficient including extrapolation for the $3d^9 4f n'l'$ (for $n' = 9$ to ∞) configurations. It must be stressed that in these computations, the only radiative stabilizing decays taken into account are those to $3d^{10}n''l''$. Further work is now under progress to include the effects of cascades. Figure 3 shows results of the DR computations for $0 < kT_e < 600$ eV. For $0 < kT_e < 200$ eV the contribution of the $3d^9 4l 4l'$ complex is dominant. For 200 eV $< kT_e <$ 400 eV, the contribution of $3d^9 4l 5l'$ is of the same order of magnitude as that of $3d^9 4l 4l'$.

$3d^{10}4s$–$3d^9 4s 4f$ LINE INTENSITIES

Using the data for DR and EA rates, an attempt is made to model the intensity of the lines emitted from inner-shell excited levels, in particular the resonant $3d^{10}4s$–$3d^9 4s 4f$ transitions in Mo XIV. One points out that, whereas the $3d^{10}4s$–$3d^9 4s 4p$ transitions have been systematically studied all along the isoelectronic sequence,[10,11] the resonant $3d^{10}4s$–$3d^9 4s 4f$ transitions, to our best knowledge have not yet been observed in elements with $Z < 49$. For heavier elements, the $3d^{10}4s$–$3d^9 4s 4f$ transitions have been observed as a Spin Orbit Split Array in the spectra emitted by laser-produced plasmas.[3,12] This has been correlated to the fact that, for low-Z elements, the upper levels of these transitions are autoionizing.[13]

At coronal conditions, in which the electron density is low enough, most of the ions are in their ground states, and electron impact deexcitation is negligible in comparison with radiative decay. A level j of the $3d^9 4s 4f$ configuration is populated by electron impact excitation from the ground state $3d^{10}4s$ (g) of the CuI-like ion, and through the capture of an electron by a NiI-like ion in the ground state $3d^{10}$ (k). In steady state one can thus write:

$$n_g n_e Q_{gj} + n_k n_e \beta_{kj} = n_j \left(\sum_i A_{ji} + \sum_{k'} A^a_{jk'} \right). \tag{5}$$

Here n_g, n_k and n_j are the ion densities in levels g, k and j respectively. The intensity of a spectral line arising from a transition $j \rightarrow g$ to the ground state is proportional to $n_j A_{jg}$. One can define a "reduced intensity" I_{jg} of the line as:

$$I_{jg} = \frac{n_j A_{jg}}{n_e n_g} = \left(Q_{gj} + \frac{n_k}{n_g} \beta_{kj} \right) \times \frac{A_{jg}}{\sum_i A_{ji} + \sum_{k'} A^a_{jk'}}. \tag{6}$$

One can write a similar expression for the reduced intensity of a line $k' \rightarrow k$ of the NiI-like $3d^{10}$–$3d^9 4f$ transition. Since the upper levels of these transitions are not autoionizing, there is no contribution of DR processes to the intensity of the line:

$$I_{k'k} = \frac{n_{k'} A_{k'k}}{n_e n_g} = \frac{n_k}{n_g} Q_{kk'} \frac{A_{k'k}}{\sum_{k''} A_{k'k''}}. \tag{7}$$

First let us assume $kT_e = 100$ eV and $n_g = n_k/4$. This electron temperature is approximately the electron temperature T_{Cu} corresponding to the most abundance of the CuI-like ions predicted in a coronal model in steady-state.[4] This relatively low temperature compared to the ionization energy ($E_I = 301$ eV) is due to the EA processes which shift T_{Cu} towards lower temperatures.[4] This model predicts that at this electron temperature, n_g is about four times smaller than n_k. For Mo XIV, the calculated average energy E_C for the $3d^{10}4s$–$3d^9 4s 4f$ transitions is found to be 336 eV. Thus the average value of the free electron energy ΔE_j appearing in Eq. (3) is 35 eV. For these temperature and densities, the computations show that the recombination process is favored over the inner-shell excitation. Figure 4(a) shows the reduced line intensities calculated at these conditions. In this figure, the CuI-like lines shown are the strongest ones only, for which $g_j A_{ji} > 10^{12}\ s^{-1}$; these transitions contribute 90% of the total transition array intensity. In the present case, about 95% of the CuI-like array intensity arise from DR processes. However, even at this low electron temperature, the total intensity of this array is still 26 times lower than the intensity of the parent NiI-like $3d^{10}$–$3d^9 4f$ line array, although these parent lines can be excited by electron collision only.

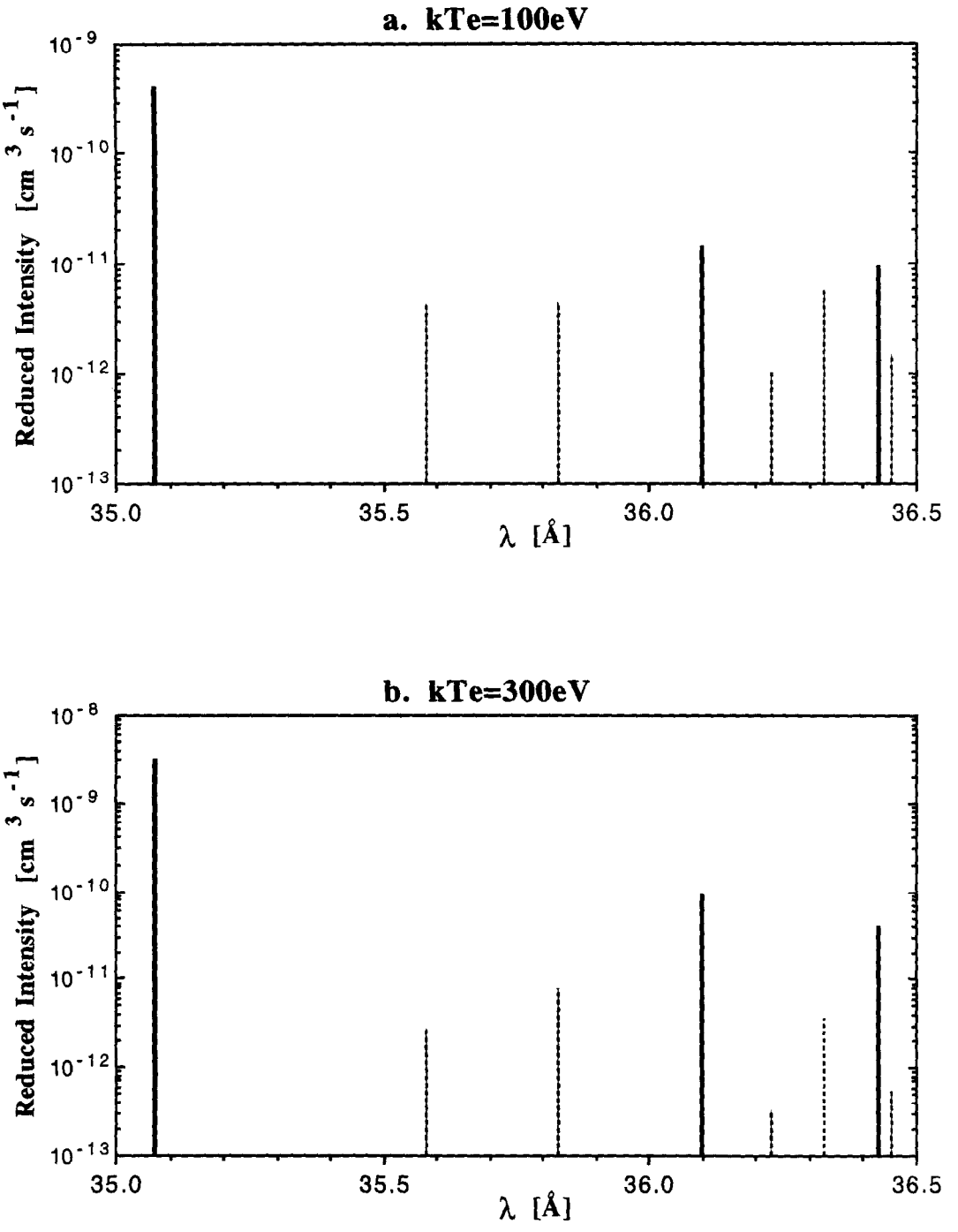

Fig. 4. Synthetic spectra (in reduced intensity) of the $3d$–$4f$ transitions in NiI-like (solid lines) and CuI-like (dotted lines) Molybdenum assuming $n_g = n_k/4$, at $kT_e = 100$ eV (a) and $kT_e = 300$ eV (b).

In a transient ionization plasma, however, where $T_e > T_{Cu}$, the electron impact excitation processes are favored. The calculations show that the DR processes contribute less than the collisional excitation to the total intensity of the CuI-like line array. The results of these calculations are shown in Fig. 4(b) which is similar to Fig. 4(a) except that $kT_e = 300$ eV. In this case, the intensity of the CuI-like line array is about 220 times weaker than the intensity of the parent NiI-like lines.

In summary, in the coronal conditions [Fig. 4(a)], most of the intensity of the CuI-like lines comes from DR processes. In a transient ionization regime [Fig. 4(b)], as in the vacuum spark,[15] the intensity of the most intense CuI-like line is about five times weaker than the weakest NiI-like line. In this regime, the DR rate coefficient is only 20% of the inner-shell excitation rate coefficient.

It must be stressed that the total rate coefficient for excitation Q and for spontaneous emission A for the $3d$–$4f$ transitions are about the same in the NiI-like and CuI-like ions, and the difference in intensities cannot be attributed to the distribution of the A-values among a greater number of lines in the CuI-like case. Indeed, the calculations show that the A-value of the most intense CuI-like line is about 40% of the A-value of the strongest NiI-like line. Instead, the great difference in intensity must be attributed to the large depopulation of the CuI-like $3d^9 4s4f$ levels via autoionization processes compared to radiative decay. This is reflected by the factor $B^r_{jg} = A_{jg}/[\Sigma A_{ji} + \Sigma A^a_{jk}]$ appearing in the line intensity, Eq. (6), and which is very small in Mo XIV. This factor is the branching ratio for radiative decay through the transition $j \rightarrow g$. This factor has been computed for each line of the transitions shown in Fig. 4(a) and 4(b).

One can also define the branching ratio for radiative decay from level j to any low level i: $B^r_j = \Sigma A_{ji}/[\Sigma A_{ji} + \Sigma A^a_{jk}]$; this branching ratio gives the relative importance of the radiative decay processes compared to the autoionization processes from the level j. For a transition array between two configurations C and C' we suggest a definition of an A-value weighted average of B^r_j as follows:

$$\bar{\rho}(C \rightarrow C') \frac{\sum_{j \in C} \sum_{i \in C'} B^r_j \times g_j A_{ji}}{\sum_{j \in C} \sum_{i \in C'} g_j A_{ji}}. \tag{8}$$

This factor gives a simple approximation of the intensity quenching of a whole transition array due to the autoionization channels. For the CuI-like transitions considered here, C being $3d^9 4s4f$ and C' $3d^{10}4s$, one obtains $\bar{\rho} = 0.03$. For the corresponding NiI-like $3d^{10}$–$3d^9 4f$ transition array: $\bar{\rho} = 1$ (since the upper levels are not autoionizing). This effect of intensity quenching of the transitions by autoionization in Mo XIV is confirmed by the absence of these lines in the experimental spectra of Mo emitted by a vacuum spark,[14] whereas the $3d^{10}4s$–$3d^9 4s4p$ transitions are well observed.

CONCLUSION

Extensive computations of EA and DR rates have been performed along the CuI and NiI isoelectronic sequences respectively. These new results are presented and discussed here for the specific case of Mo XIV. These calculations show that at coronal equilibrium, the Mo XIV $3d^{10}4s$–$3d^9 4s4f$ line array is about 26 times weaker than the parent $3d^{10}$–$3d^9 4f$ lines in Mo XV. In transient ionization regime, the intensity ratio can reach even smaller values (about 1/200 at $kT_e = 300$ eV). This is due to the intensity quenching of the transitions by autoionization in Mo XIV, whose effect can be evaluated by an average radiative branching ratio $\bar{\rho}$.

Acknowledgements—The authors thank A. Bar Shalom and J. Oreg of the University of the Negev at Beer-Sheva, Israel, and W. H. Goldstein of LLNL for fruitful discussions and for making available the latest versions of the HULLAC package.

REFERENCES

1. R. A. London, M. D. Rosen, and J. E. Trebes, *Appl. Opt.* **28,** 3397 (1989).
2. J. Bruneau, C. Chenais-Popovics, D. Desenne, J. C. Gauthier, J. P. Geindre, M. Klapisch, J. P. Le Breton, M. Louis-Jacquet, D. Naccache, and J. P. Perrine, *Phys. Rev. Lett.* **65,** 1435 (1990).
3. M. Klapisch, P. Mandelbaum, A. Zigler, C. Bauche-Arnoult, and J. Bauche, *Phys. Scripta* **34,** 51 (1986).
4. D. Mitnik, P. Mandelbaum, J. L. Schwob, A. Bar-Shalom, J. Oreg, and W. H. Goldstein, *Phys. Rev. A* **50,** 4911 (1994).
5. M. Klapisch, A. Bar Shalom, and W. H. Goldstein, The HULLAC code for atomic physics. Unpublished (1988).
6. M. Klapisch, J. L. Schwob, B. Fraenkel, and J. Oreg, *J. Opt. Soc. Am.* **67,** 148 (1977).
7. J. Oreg, W. H. Goldstein, M. Klapisch, and A. Bar Shalom, *Phys. Rev. A* **44,** 1750 (1991).
8. A. Bar Shalom, M. Klapisch, and J. Oreg, *Phys. Rev. A* **38,** 1733 (1988).

9. W. Lotz, *Z. Phys.* **206,** 205 (1967); **216,** 241 (1968); **232,** 101 (1970).
10. J. F. Wyart, J. Reader, and A. Ryabtsev, *J. Opt. Soc. Am.* **71,** 692 (1981).
11. M. Klapisch, P. Mandelbaum, J. L. Schwob, A. Bar Shalom, and N. Schweitzer, *Physics. Lett.* **84A,** 177 (1981).
12. A. Zigler, P. Mandelbaum, J. L. Schwob, and D. Mitnik, *Phys. Scripta* **50,** 61 (1994).
13. P. Mandelbaum, in *Atomic Processes in Plasmas*, E. S. Marmar and J. L. Terry, eds., p. 86 (1992).
14. N. Schweitzer, Ph.D. thesis, The Hebrew University of Jerusalem (1978).
15. J. L. Schwob and B. S. Fraenkel, *Phys. Lett.* **40A,** 81 (1972).